

## Research Article

## Discovery and characterization of novel paramyxoviruses from bat samples in China

Haoxiang Su<sup>a,1</sup>, Yuyang Wang<sup>a,1</sup>, Yelin Han<sup>a,1</sup>, Qi Jin<sup>a,\*</sup>, Fan Yang<sup>a,\*</sup>, Zhiqiang Wu<sup>a,b,\*</sup><sup>a</sup> NHC Key Laboratory of Systems Biology of Pathogens, Institute of Pathogen Biology, Chinese Academy of Medical Sciences & Peking Union Medical College, Beijing, 100730, China<sup>b</sup> Key Laboratory of Respiratory Disease Pathogenomics, Chinese Academy of Medical Sciences & Peking Union Medical College, Beijing, 100730, China

## ARTICLE INFO

## Keywords:

Paramyxovirus  
*Jeilongvirus*  
Bat  
Host and region switches  
China

## ABSTRACT

Many paramyxoviruses are responsible for a variety of mild to severe human and animal diseases. Based on the novel discoveries over the past several decades, the family *Paramyxoviridae* infecting various hosts across the world includes 4 subfamilies, 17 classified genera and 78 species now. However, no systematic surveys of bat paramyxoviruses are available from the Chinese mainland. In this study, 13,064 samples from 54 bat species were collected and a comprehensive paramyxovirus survey was conducted. We obtained 94 new genome sequences distributed across paramyxoviruses from 22 bat species in seven provinces. Bayesian phylodynamic and phylogenetic analyses showed that there were four different lineages in the *Jeilongvirus* genus. Based on available data, results of host and region switches showed that the bat colony was partial to interior, whereas the rodent colony was exported, and the felines and hedgehogs were most likely the intermediate hosts from *Scotophilus* spp. rather than rodents. Based on the evolutionary trend, genus *Jeilongvirus* may have originated from *Mus* spp. in Australia, then transmitted to bats and rodents in Africa, Asia and Europe, and finally to bats and rodents in America.

## 1. Introduction

Emerging infectious diseases pose serious threats to global economy, security and public health. Most human pathogens, including Marburg virus, Nipah virus, Hendra virus, Ebola virus, severe acute respiratory syndrome coronavirus (SARS-CoV), Middle East respiratory coronavirus (MERS-CoV), SARS-CoV-2 and others, have animal origins and arose through cross-species transmission (Lau et al., 2005; Leroy et al., 2005; Memish et al., 2013; Smith and Wang, 2013; Swanepoel et al., 2007; Wang et al., 2006). These viruses probably originate from bat, the second most diverse mammalian order after rodent, comprising approximately 22% of all named mammal species (Letko et al., 2020). Bats are widely distributed geographically, have extensive species diversity and have unique behavior such as flight patterns, long life spans, gregarious roosting and mobility behaviors. Bats also have intimate interactions with human and livestock, regarded as natural reservoirs for a diverse pool of viruses and deserved to be studied in depth (Calisher et al., 2006; Drexler et al., 2012; Halpin et al., 2011).

Paramyxoviruses are a group of large enveloped viruses with negative-sense single-stranded RNA (14,296–20,148 nt in length)

infecting mammals, birds, reptiles and fish (Rima et al., 2019). Many paramyxoviruses, including Nipah virus, Hendra virus, Menangle viruses, measles virus, mumps virus and parainfluenza viruses, are responsible for a variety of mild to severe human and animal diseases (Bowden et al., 2012; Branche and Falsey, 2016; Henrickson, 2003; Hviid et al., 2008; Marsh and Wang, 2012; Middleton, 2014; Moss, 2017). The family *Paramyxoviridae* includes 4 subfamilies (*Avulavirinae*, *Metaparamyxovirinae*, *Orthoparamyxovirinae* and *Rubulavirinae*), 17 classified genera, 78 species and many unclassified viruses (International Committee of Taxonomy of Viruses, ICTV; <https://talk.ictvonline.org/>). Over the past two decades, novel paramyxoviruses have sprung up in various hosts, including rodents (Alkhovsky et al., 2018; Lambeth et al., 2009; Larsen et al., 2021; Lee et al., 2021; Miller et al., 2003; Vanmechelen et al., 2018, 2021; Woo et al., 2011), bats (Albarino et al., 2014; Baker et al., 2020; Burroughs et al., 2015; de Souza et al., 2021; Johnson et al., 2018; Larsen et al., 2021; Lau et al., 2010; Marsh et al., 2012; Noh et al., 2018), snakes (Hyndman et al., 2012), pigs (Lau et al., 2013), cats (Choi et al., 2020; Sakaguchi et al., 2020; Sieg et al., 2015), squirrels (Brooks et al., 2014; Forth et al., 2018), goats (Li et al., 2014), cattle (Leal et al., 2019), hedgehogs (Vanmechelen et al., 2020) across the world. These

\* Corresponding authors.

E-mail addresses: [zdsys@vip.sina.com](mailto:zdsys@vip.sina.com) (Q. Jin), [yymf129@163.com](mailto:yymf129@163.com) (F. Yang), [wuzq2009@ipbcams.ac.cn](mailto:wuzq2009@ipbcams.ac.cn) (Z. Wu).<sup>1</sup> Haoxiang Su, Yuyang Wang, and Yelin Han contributed equally to this work.

discoveries significantly increased from the family initially identified as having five genera to the multiple genera known today.

Although sporadic studies contributed to this abundant list, no systematic surveys of bat paramyxoviruses are available for the Chinese mainland. Our team has conducted perennial viral surveys on rodents and bats across China and Southeast Asia to monitor and discover the potential zoonotic viral pathogens (Wu et al., 2018, 2021). We established two continuously updated online virome databases, DBatVir (Chen et al., 2014) and DRodVir (Chen et al., 2017), and discovered Mojiang virus (Wu et al., 2014) of *Henipavirus* genus from rodents (*Rattus flavipectus*) in 2012 and Bat Ms-ParaV/Anhui2011 (Wu et al., 2016) of *Jeilongvirus* genus from bats (*Miniopterus schreibersii*) in 2016. Between 2016 and 2021, more than 13,000 samples from 54 bat species were collected and underwent a comprehensive virome survey. Based on preliminary work and existing resources, a retrospective study surveying paramyxoviruses was performed on multi-bat species sampled in China. The identification of diverse paramyxoviruses, as well as the new characterizations of their genome organizations, RNA editing sites, transmembrane helices sites, and glycosylation sites, increased our understanding for ecological distribution of bat paramyxoviruses in China, and spurred us to further investigate the host and region switches of such viruses.

## 2. Materials and methods

### 2.1. Sample collection

Between 2016 and 2021, a total of 13,064 samples from 54 bat species were collected from 703 sampling sites in fourteen provinces (Guangxi, Guangdong, Yunnan, Sichuan, Hubei, Hainan, Zhejiang, Jiangxi, Guizhou, Hunan, Liaoning, Fujian, Anhui and Chongqing) as described previously (Wu et al., 2022). The captured bat species were initially determined from morphological features and subsequently confirmed using patagium with barcoding of mitochondrial cytochrome *b*. The sampling locations were recorded by geographic names and GPS coordinates of latitude and longitude. The swab samples of pharyngeal and anal in triplicate were immersed in virus sampling tubes (Yocon, China) with maintenance medium, temporarily stored at  $-20^{\circ}\text{C}$ , transported to the laboratory and stored at  $-80^{\circ}\text{C}$ .

### 2.2. Library construction and next generation sequencing

According to the bat species and the sampling sites, the swab samples were pooled by adding 1 mL of each maintenance medium into one new container. The pooled samples were then processed with a virus-particle-protected nucleic acid purification method used in previous research (Wu et al., 2012). The samples were centrifuged at  $10,000\times g$  for 10 min to precipitate the impurities. The supernatants were filtered through a  $0.45\ \mu\text{m}$  polyvinylidene difluoride filter (Millipore, Germany) to remove eukaryotic and bacterial-sized particles. Then the filtered samples were centrifuged at  $100,000\times g$  for 3 h at  $4^{\circ}\text{C}$ . The pellets re-suspended in Hank's balanced salt solution were digested in a cocktail of DNase and RNase enzymes (Turbo DNase, Ambion, USA; Benzonase, Novagen, Germany and RNase One, Promega, USA) to remove naked DNA and RNA at  $37^{\circ}\text{C}$  for 2 h. The viral nucleic acids were extracted using a QIAmp MinElute Virus Spin Kit (Qiagen, USA). The first-strand viral cDNA was synthesized using the primer K-8N and a SuperScript™ III First-Strand Synthesis system (Invitrogen, USA). The cDNA was further converted into double-stranded cDNA (ds cDNA) with a Klenow fragment (NEB, United States) at  $37^{\circ}\text{C}$  for 1 h. Sequence-independent PCR amplification was performed using primer K. The PCR fragments which are from 300 to 2000 bps were extracted by magnetic beads (Beckman Coulter, USA). The purified products were quality checked by Agilent 2100 and then mixed at equal molar concentrations. Libraries were constructed using the Nextera® XT DNA Sample Preparation Kit (Illumina, USA) according to the manufacturer's instructions, and sequenced with an Illumina HiSeq

X Ten sequencer for a paired-end read of 150 bp. The sequence reads were filtered as previous criteria described (Yang et al., 2011). Clean data were generated after adaptor sequence, primer K sequence, and low-quality reads were removed.

### 2.3. Taxonomic assignment and genome assembly

The valid sequence reads were aligned to sequences in the NCBI non-redundant nucleotide database (NT) and non-redundant protein database (NR) using BLASTn and BLASTx, respectively. The taxonomies with the best BLAST scores (E score  $<10^{-5}$ ) were parsed by MEGAN6. Extracted paramyxovirus reads were assembled by megahit v1.2.9 and the assembled sequences were used as references during genome sequencing.

### 2.4. Genome sequencing

The assembled contigs of paramyxoviruses and their closest reference sequence were identified by BLAST. The partial genomes were amplified with nested specific primers. The PCR product, between 1500 bp and 2000 bp, were gel purified and then sequenced. The remaining genomic sequences were determined using genome walking, 5' and 3' rapid amplification of cDNA ends (RACE). The ORFs of complete sequenced viruses were predicted with the ORFfinder of NCBI (<https://www.ncbi.nlm.nih.gov/orffinder/>).

### 2.5. Bayesian phylodynamic analysis

Aside from sequences obtained in this study, all *Jeilongvirus* sequences from GenBank were added to our dataset. The conserved region of 99 amino acids related to target fragment of universal primer was used as query for BLASTx, and then a total of 353 *Jeilongvirus* sequences were found. After removing redundant sequences with high identity from the same host and the same collection location, a total of 127 sequences were finally used for Bayesian phylogenetic analysis. Multiple sequence alignments of the nucleotide sequences were performed using MAFFT v7.475 (Katoh and Standley, 2013) followed by TrimAL to trim sequences. TempEst (Rambaut et al., 2016) was used to assess the temporal structure within datasets. The datasets did not contain enough temporal signals to estimate substitution rates and the most recent common ancestor (TMRCA), therefore tip dates were not used. The best-fitting combination of substitution models GTR + Gamma (4) + Invariant nucleotide substitution model were selected according to the calculated result of ModelFinder (Kalyaanamoorthy et al., 2017). The analysis was run to select strict/lognormal uncorrelated relaxed clock, and coalescent models (constant population size/exponential growth/GMRF Bayesian Skyride). Host family and sampling region were reconstructed for the ancestral state of each node in the phylogenetic tree for two discrete traits and a symmetric trait substitution model was applied for BSSVS analysis. The BSSVS was applied to estimate the significance of pairwise switches between trait states using Bayes Factors (BF) computed in Spread3 (Bielejec et al., 2016) as a measure scale of statistical significance (Lemey et al., 2009). BF support scale was interpreted according to Jeffreys (1961). All  $\text{BF} > 3$  states were presented through TBtools (Chen et al., 2020). Model combinations were compared, and the best-fitting model was selected using a Path sampling/stepping-stone sampling analysis (Baele et al., 2012, 2013). Finally, a lognormal uncorrelated relaxed clock and a constant population size coalescent model. Each analysis was run for  $5 \times 10^7$  generations in BEAST v1.10.4 (Suchard et al., 2018), with sampling every  $5 \times 10^3$  steps. Convergence of the chain was visualized in Tracer v1.7.1 (Rambaut et al., 2018) and the effective sample size (ESS) of main parameters was greater than 200 after discarding the first 10% of the chain as burn-in. TreeAnnotator was used to summarize posterior tree distributions and annotated the estimated values to a maximum clade credibility (MCC) tree with a burn-in of 10%, which was visualized using FigTree v1.4.4. To assess the phylogenetic relationships among *Jeilongvirus*, a Haplotype Network was constructed with the last 100bp of 353 *Jeilongvirus* dataset using PopART

through TCS network program. After combining redundant identical sequences, 274 kinds of haplotype were left.

### 2.6. Identity and phylogenetic analysis

The percent identity of the nucleotide and deduced amino acid sequences was assessed using MegAlign (DNA Star package Lasergene v.7.0.1). Phylogenetic analysis of the complete L protein amino acid sequences was performed using the maximum likelihood (ML) method available in iqtree (Nguyen et al., 2015) with 1000 UltraFastbootstrap (Hoang et al., 2018) replicates, employing the best-fit model LG+F+I+G4 chosen according to Bayesian Information Criterion (BIC) in ModelFinder (Kalyaanamoorthy et al., 2017). The resulting phylogenetic trees were visualized using Figtree v1.4.4.

### 2.7. Transmembrane helices and glycosylation site analysis

The amino acid sequences were used for predicting, the complete SH, TM and X genes for prediction of transmembrane helices with TMHMM, the complete F and G genes for prediction of N-linked glycosylation sites and O-GalNAc (mucin type) glycosylation sites with NetNGlyc 1.0 and NetOGlyc 4.0, respectively (<https://services.healthtech.dtu.dk/>).

### 2.8. Accession numbers

All genome sequences were submitted to GenBank. Accession numbers for the viruses are ON263473 to ON263566.

## 3. Results

### 3.1. Virome and prevalence analysis for paramyxoviruses

A total of 40 sequences of bat paramyxoviruses were identified in 14 provinces and the Macao special administrative region of China and recorded in DBatVir and GenBank, thereinto 16 sequences originated from our previous study (Wu et al., 2016) (Supplementary Table S1). The 36 sequences were found from 15 bat species, while 4 belonged to the *Orthorubulavirus* genus of *Rubulavirinae* subfamily from Guangdong, Shanxi and Jilin provinces; 4 belonged to the *Pararubulavirus* genus of *Rubulavirinae* subfamily from Guangdong and Yunnan provinces; 1 belonged to the *Henipavirus* genus of *Orthoparamyxovirinae* subfamily from Yunnan Province; 27 belonged to the *Jeilongvirus* genus of *Orthoparamyxovirinae* subfamily. The other 4 sequences belonged to the *Orthoavulavirus* genus of *Avulavirinae* subfamily found in unclassified *Chiroptera* from Guangxi Province.

In this study, 13,064 samples from bats were pooled and applied for next generation sequencing as described previously (Wu et al., 2022). Meanwhile, a total of 760.3 GB of nucleotide clean data with 1,718,361,529 valid reads was obtained from next generation sequencing. Among them, 612,529 reads (~0.036% of the total sequence reads) were matched with paramyxovirus proteins available in the NCBI NR database, and 291 out of 372 pools were found to be paramyxovirus-positive. The proportion of paramyxovirus-related reads in each pool varied from 0.00016% to 73.66%. Based on assembled contigs and nested specific primers, the PCR results confirmed that 65 out of total 372 pools were positive for paramyxovirus. Ninety-four new genome sequences distributed across paramyxovirus were obtained experimentally from 22 bat species in seven provinces (Guangdong, Guangxi, Yunnan, Hainan, Jiangxi,



**Fig. 1.** Geographical distribution of bat paramyxovirus sequences in China. The red color representing the provinces changes according to the numbers of sequences found. The outer rings represent the bat species that the sequences discovered and are proportional to the numbers. The inner pie charts represent the numbers of sequences found, white partial is the sequences found previously, and blue partial is the sequences found during this study. AH, Anhui; GD, Guangdong; GX, Guangxi; HB, Hubei; HI, Hainan; JL, Jilin; JX, Jiangxi; LN, Liaoning; SC, Sichuan; SN, Shaanxi; SX, Shanxi; XZ, Tibet; YN, Yunnan; QH, Qinghai; ZJ, Zhejiang.

Hubei and Zhejiang) (Supplementary Table S2). Only one strain sequence BtEsp-ParaV/YN2017A, a 336 nt fragment of phosphoprotein gene, was determined to belong to the *Orthorubulavirus* genus of *Rubulavirinae* subfamily, the other 93 sequences belonged to the *Jeilongvirus* genus of *Orthoparamyxovirinae* subfamily.

In total, by combining current study data with published data, 134 sequences were discovered from 31 bat species and unclassified *Chiroptera* spp. in sixteen provinces and the Macao special administrative region of China (Fig. 1).

### 3.2. Derivation of global evolution trend

By using sequence alignment analysis in GenBank, the phylogenetic reconstruction of 127 partial Large protein (L) sequences based on the consensus degenerate primers (Tong et al., 2008) (PAR-F/R) was conducted. The more obvious clustering trend of the maximum clade credibility (MCC) tree was shown along with more sequences, bat species and regions (Fig. 2). All *Jeilongvirus* could be divided into four main lineages: (1) lineage 1 (L1), all the bat-borne paramyxoviruses formed a well-supported monophyletic cluster associated with the previously proposed *Shaanvirus* genus and distributed in Asia, North America and Africa;

(2) lineage 2 (L2), contained rodent-borne paramyxoviruses across the world, with feline-borne paramyxoviruses from Germany and Japan evolving later in time; (3) lineage 3 (L3), with surprisingly more members, included bat-borne paramyxoviruses in multiple species from Asia alone, hedgehog-borne paramyxoviruses from Europe, and rodent-borne paramyxoviruses from North America and Africa; (4) lineage 4 (L4), covered North America and South America from bat-borne paramyxoviruses only. The viruses identified in this study were distributed in L1 and L3.

A total of 274 kinds of haplotype with different individual sizes were used in network construction (Supplementary Fig. S1). The evolutions of bats among L1, L3 and L4 with rodents between L2 and L3 were intertwined rather than independent. The bat colony and rodent colony were aggregated, but the bat colony was invaded by some rodent populations. The seven species of *Jeilongvirus* in ICTV were not the ancestral viruses and leaned to the tips of tendency.

### 3.3. Host and region switches

A Bayesian stochastic search variable selection (BSSVS) procedure was used to identify the host and region switches of *Jeilongvirus* among bats,

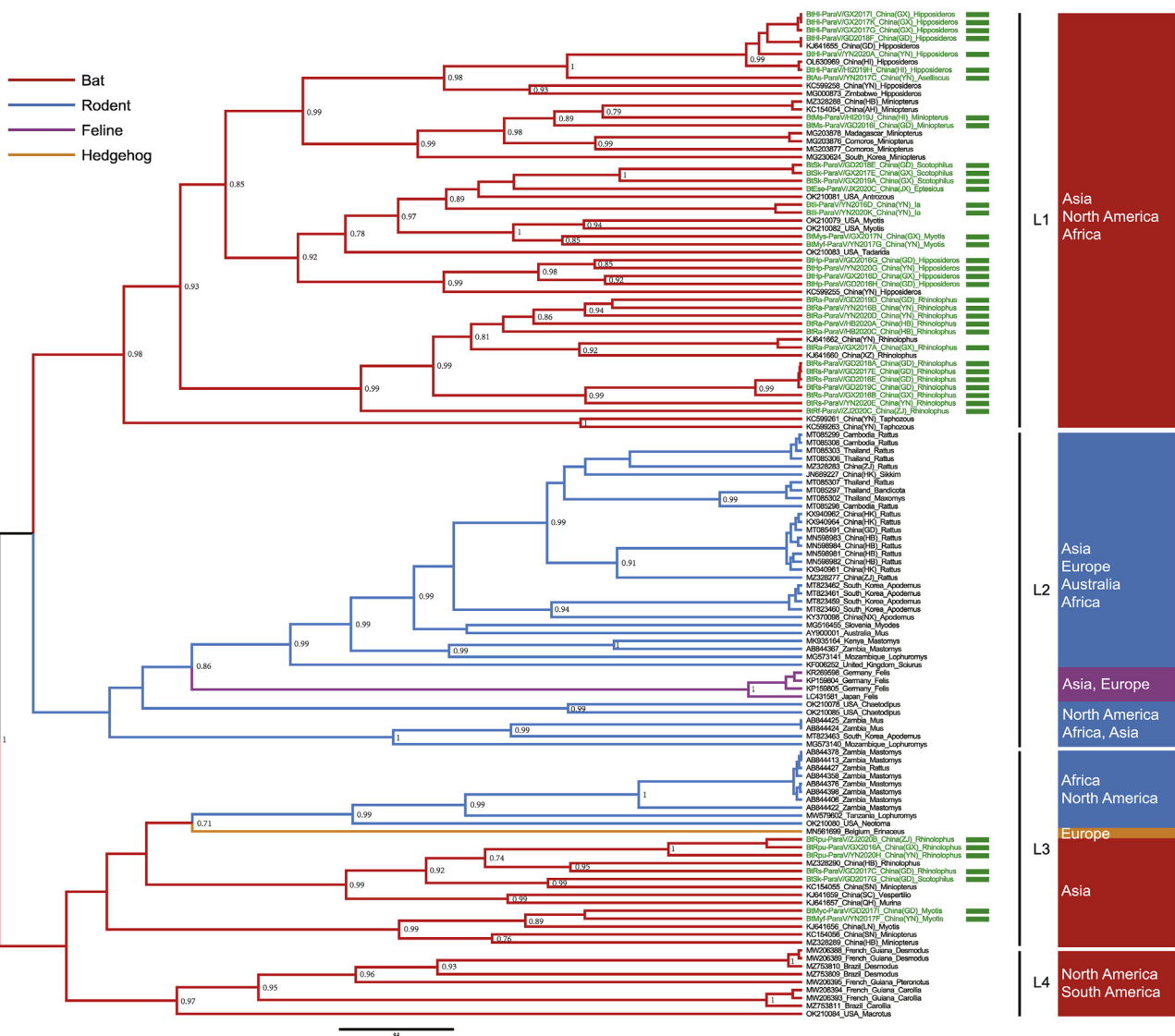
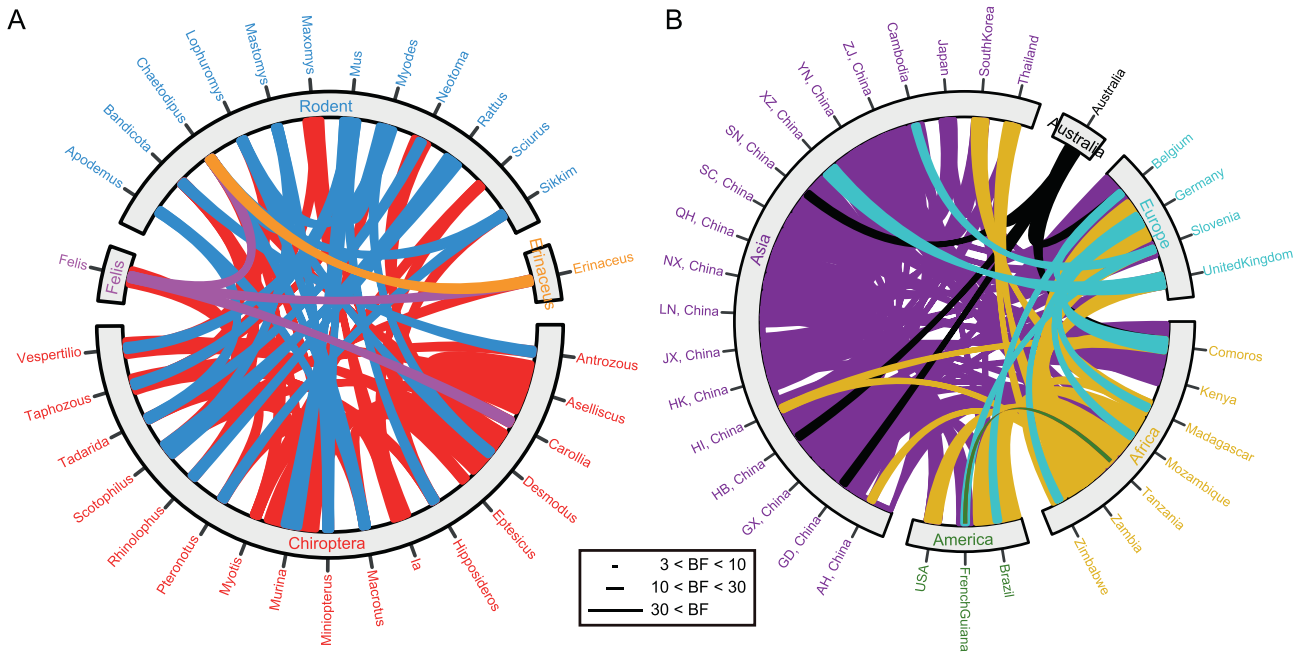


Fig. 2. Evolution overview of *Jeilongvirus*. The maximum clade credibility tree is inferred from partial L sequences. Sequences from bats are labeled in red, rodent sequences are labeled in blue, feline sequences are labeled in violet, and hedgehog sequence is labeled in yellow. The viruses identified in this study are labeled by green rectangles.



**Fig. 3.** The switch maps. **A** Host switches. Bats are labeled in red, rodents are labeled in blue, felines are labeled in violet, and hedgehog is labeled in yellow. **B** Region switches. Asia is labeled in violet, Australia is labeled in black, Europe is labeled in wathet blue, Africa is labeled in yellow, and America is labeled in green. The length of lines represents the value of Bayesian factors (ZJ, Zhejiang; YN, Yunnan; XZ, Tibet; SN, Shaanxi; SC, Sichuan; QH, Qinghai; NX, Ningxia; LN, Liaoning; JX, Jiangxi; HK, Hong Kong; HI, Hainan; HB, Hubei; GX, Guangxi; GD, Guangdong; AH, Anhui).

rodents, felines and hedgehogs with the above *L* sequences. Bayesian factors (BF) were calculated to estimate the significance of switches (Fig. 3).

Two very strong support (BF > 30), eight strong support (10 < BF < 30) and fifty-five substantial support (3 < BF < 10) switches for host were identified (Fig. 3A and Supplementary Table S3). From *Murina* and *Aselliscus* to *Desmodus* within bats were super supported. The host switches were frequent, but bats were partial to interior, and rodents were exported based on the trend. The *Mus* spp. transmitted to *Myodes* spp. of rodents, and to *Murina*, *Taphozous*, *Hipposideros*, *Miniopterus*, *Vespertilio* spp. of bats, but did not receive from others; the *Rattus* spp. to *Scotophilus* and *Rhinolophus* spp. of bats; the *Mastomys* spp. to *Chaetodipus* spp. of rodents and *Miniopterus*, *Scotophilus* spp. of bats. Only one route could connect the four hosts from *Scotophilus* spp. to *Felis*, to *Erinaceus*, to *Chaetodipus* spp. The *Scotophilus* spp. could transmit to *Felis*, *Erinaceus* and *Chaetodipus* spp., the *Felis* spp. to *Erinaceus* and *Chaetodipus* spp., but the *Erinaceus* spp. only to *Chaetodipus* spp.

Seventeen very strong support (BF > 30), thirty-six strong support (10 < BF < 30) and sixty-seven substantial support (3 < BF < 10) switches for region were identified (Fig. 3B and Supplementary Table S4). Each within and among with Africa, Asia, Europe were exchanged frequently. Only Australia was the donor to Africa, Asia and Europe. America received from Africa, Asia and Europe, but exported just once from Guiana to Tanzania with generally supported (BF = 3.19). The *Mus* spp. came from Australia and Africa; the *Rattus* spp. from Africa and Asia; the *Mastomys* spp. from Africa; the *Scotophilus* spp. from Asia; the *Felis* spp. from Asia and Europe; the *Erinaceus* spp. from Europe; the *Chaetodipus* spp. from America.

### 3.4. Discovery of novel paramyxoviruses and phylogenetic analysis

Combining with the reference complete genomes from rodents, bats, hedgehogs and felines of recently studies proposed to *Jeilongvirus*, 17 novel representative sequences with complete or nearly complete genomes were selected for analysis. Using the complete *L* gene of the above sequences, phylogenetic reconstruction was conducted. As shown in Fig. 4A, the analysis of *Jeilongvirus* was the same as the evolutionary trend above. The L1 and L4 had bat species-specificity. L1 contained 16 novel

paramyxoviruses in this study and 1 species in ICTV. L4 had three novel bat paramyxoviruses in Brazil that were previously suggested establishing a putative novel genus named *Macrojevirus* (de Souza et al., 2021) of *Orthoparamyxovirinae* subfamily. Both L2 included six rodent species in ICTV and L3 included one novel bat paramyxovirus in this study had different host sources.

### 3.5. Genome organization of novel bat paramyxoviruses

Based on phylogenetic analysis of the complete *L* gene, host range and biochemical criteria, the 17 new discoveries and recently studies of complete genomes proposed to the genus *Jeilongvirus* could be divided into four lineages with some special characterizations (Fig. 4B, Table 1 and Table 2).

The L1 contained *Miniopteran jeilongvirus* discovered and isolated from *Miniopterus schreibersii*, together with discoveries from *Hipposideros larvatus*, *Hipposideros armiger*, *Ia io*, *Scotophilus kuhlii*, *Rhinolophus sinicus*, *Rhinolophus affinis* and *Hipposideros pomona*. All L1 had eight ORFs with the order 3'-N-P-M-F-SH-TM-G-L-5' consistent with *Beilong jeilongvirus*, *Tailam jeilongvirus*, *Jun jeilongvirus* and *Myodes jeilongvirus*. The SH and TM ORFs of above four *Jeilongvirus* species varied from 69 to 82 and 254 to 258 amino acids; 210 to 249 and 765 to 777 nucleotides, however the L1 were longer from 216 to 277 and 419 to 561 amino acids; 651 to 834 and 1260 to 1686 nucleotides. The RNA editing site for processing the V or W protein conserved in the *P* gene sequence of rodent-borne and feline-borne *Jeilongvirus* of the L2 was 'TTAAAAAAGGCA', but the L1 was completely replaced by 'TTAAAAAACCA'. Six novel discoveries of different bat species in L1 were used to compare with four lineages of *Jeilongvirus*, *Hendra henipavirus*, *Feline morbillivirus* and *Tupaia narnovirus*, which shared 40.6%–66.1% aa identities in N, 26.1%–63.3% in P, 46.8%–77.9% in M, 36.7%–55.4% in F, 21.4%–50.1% in SH, 21.1%–35.8% in TM, 19.8%–80.7% in G and 46.7%–69.6% in L.

The L3 was discovered from *Rhinolophus pusillus* in Yunnan Province of China, alongside *Belerina* paramyxovirus from hedgehogs in Belgium. The L4 included *Kanhgag* paramyxovirus, *Boe* paramyxovirus and *Guat6* paramyxovirus from *Desmodus rotundus* and *Carollia perspicillata* in

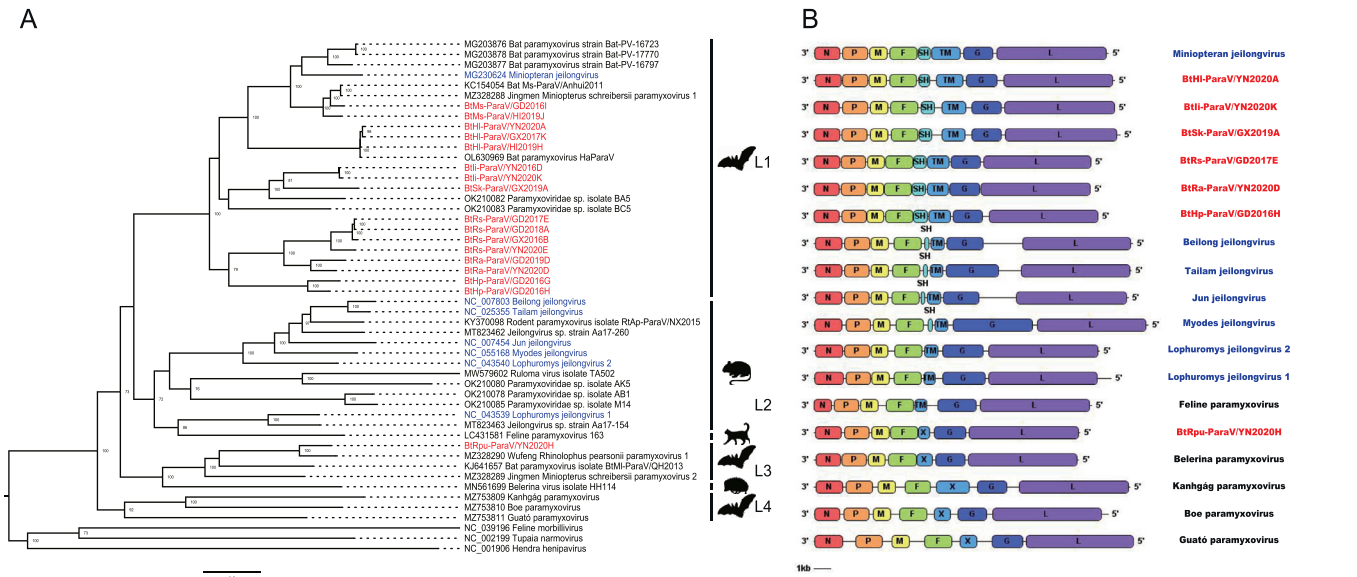


**Fig. 4.** Phylogenetic analysis and genome organization of novel bat paramyxoviruses. **A** Phylogenetic tree based on the complete L sequences of complete genomes proposed to *Jeilongvirus*. Animal silhouettes represent the paramyxovirus hosts. **B** The genome structure charts of representative paramyxovirus proposed to *Jeilongvirus* from different hosts. The viruses found in this study are labeled in red, and the seven species of *Jeilongvirus* in ICTV are labeled in blue, and the other representative members in the L2, L3 and L4 are labeled in black.

Araçatuba of Brazil that belonged to putative novel genus in 2021. All L3 and L4 had seven ORFs with the order 3'-N-P-M-F-X-G-L-5' consistent with *Lophuromys jeilongvirus 2*, *Lophuromys jeilongvirus 1* and Feline paramyxovirus. The TM ORFs of the above three varied from 218 to 275 amino acids; 657 to 828 nucleotides, and the X gene between F and G encoded from 227 to 658 amino acids; 684 to 1977 nucleotides. The RNA editing site was conserved with the L2. The BtRpu-ParaV/YN2020H shared 42.9%–58.3% aa identities in N, 28.0%–58.9% in P, 42.3%–

62.2% in M, 39.0%–56.6% in F, 13.1%–70.7% in X, 19.1%–77.1% in G and 47.4%–63.4% in L.

3.6. Transmembrane helices of SH, TM and X

The SH, TM and ORFX of four lineages were used for the prediction of transmembrane helices (Supplementary Fig. S2). The lengths of SH, TM and X proteins, the locations of the putative transmembrane regions as

**Table 1**  
Characterization of novel discoveries.

| Lineage                                  | Representative members                  | ORFs                    | The RNA editing site | Discovered from                 | Location                         |
|--|---|-------------------------|----------------------|---------------------------------|----------------------------------|
| L1                                       | MG230624 Bat-ParaV/B16-40               | 8                       | TTAAAAAACCA          | <i>Miniopterus schreibersii</i> | Danyang, Korea                   |
|  | KC154054 Bat Ms-ParaV/Anhui2011         | 8                       | TTAAAAAACCA          | <i>Miniopterus schreibersii</i> | Anhui, China                     |
|  | BtMs-ParaV/GD2016I                      | 8                       | TTAAAAAACCA          | <i>Miniopterus schreibersii</i> | Guangdong, China                 |
|  | BtMs-ParaV/HI2019J                      | 8                       | TTAAAAAACCA          | <i>Miniopterus schreibersii</i> | Hainan, China                    |
|  | BtHl-ParaV/YN2020A                      | 8                       | TTAAAAAACCA          | <i>Hipposideros larvatus</i>    | Yunnan, China                    |
|  | BtHl-ParaV/GX2017K                      | 8                       | TTAAAAAACCA          | <i>Hipposideros larvatus</i>    | Guangxi, China                   |
|  | BtHl-ParaV/HI2019H                      | 8                       | TTAAAAAACCA          | <i>Hipposideros larvatus</i>    | Hainan, China                    |
|  | OL630969 HaParaV                        | 8                       | TTAAAAAACCA          | <i>Hipposideros armiger</i>     | Hainan, China                    |
|  | Btli-ParaV/YN2016D                      | 8                       | TTAAAAAACCA          | <i>Ia io</i>                    | Yunnan, China                    |
|  | Btli-ParaV/YN2020K                      | 8                       | TTAAAAAACCA          | <i>Ia io</i>                    | Yunnan, China                    |
|  | BtSk-ParaV/GX2019A                      | 8                       | TTAAAAAACCA          | <i>Scotophilus kuhlii</i>       | Guangxi, China                   |
|  | BtRs-ParaV/GD2017E                      | 8                       | TTAAAAAACCA          | <i>Rhinolophus sinicus</i>      | Guangdong, China                 |
|  | BtRs-ParaV/GD2018A                      | 8                       | TTAAAAAACCA          | <i>Rhinolophus sinicus</i>      | Guangdong, China                 |
|  | BtRs-ParaV/GX2016B                      | 8                       | TTAAAAAACCA          | <i>Rhinolophus sinicus</i>      | Guangxi, China                   |
|  | BtRs-ParaV/YN2020E                      | 8                       | TTAAAAAACCA          | <i>Rhinolophus sinicus</i>      | Yunnan, China                    |
|  | BtRa-ParaV/GD2019D                      | 8                       | TTAAAAAACCA          | <i>Rhinolophus affinis</i>      | Guangdong, China                 |
|  | BtRa-ParaV/YN2020D                      | 8                       | TTAAAAAACCA          | <i>Rhinolophus affinis</i>      | Yunnan, China                    |
|  | BtHp-ParaV/GD2016G                      | 8                       | TTAAAAAACCA          | <i>Hipposideros pomona</i>      | Guangdong, China                 |
|  | BtHp-ParaV/GD2016H                      | 8                       | TTAAAAAACCA          | <i>Hipposideros pomona</i>      | Guangdong, China                 |
|  | L2                                      | NC_007803 Beilong virus | 8                    | TTAAAAAAGGCA                    | Human kidney mesangial cell line |
| NC_025355 Tailam virus strain TL8K       |   | 8                       | TTAAAAAAGGCA         | <i>Rattus andamanensis</i>      | Hongkong, China                  |
| NC_007454 J-virus                        |   | 8                       | TTAAAAAAGGCA         | <i>Mus musculus</i>             | Australia                        |
| NC_055168 Pohorje myodes paramyxovirus 1 |   | 8                       | TTAAAAAAGGCA         | <i>Myodes glareolus</i>         | Slovenia                         |
| L3                                       | NC_043540 Mount Mabu Lophuromys virus 2 | 7                       | TTAAAAAAGGCA         | <i>Lophuromys machangui</i>     | Mozambique                       |
|  | NC_043539 Mount Mabu Lophuromys virus 1 | 7                       | TTAAAAAAGGCA         | <i>Lophuromys machangui</i>     | Mozambique                       |
|  | LC431581 Feline paramyxovirus 163       | 7                       | TTAAAAAAGGCA         | Cat                             | Japan                            |
|  | BtRpu-ParaV/YN2020H                     | 7                       | TTAAAAAAGGCA         | <i>Rhinolophus pusillus</i>     | Yunnan, China                    |
| L4                                       | MN561699 Belerina virus isolate HH114   | 7                       | TTAAAAAAGGCA         | <i>Erinaceus europaeus</i>      | Belgium                          |
|  | MZ753809 Kanhgág paramyxovirus          | 7                       | TTAAAAAAGGCA         | <i>Desmodus rotundus</i>        | Araçatuba, Brazil                |
|  | MZ753810 Boe paramyxovirus              | 7                       | TTAAAAAAGGCA         | <i>Desmodus rotundus</i>        | Araçatuba, Brazil                |
|  | MZ753811 Guató paramyxovirus            | 7                       | TTAAAAAAGGCA         | <i>Carollia perspicillata</i>   | Araçatuba, Brazil                |

**Table 2**  
Amino acid identities.

|                                 |      | L1   |      | L2   |      |      |      | L3   |      |      | L4   |      | Henipavirus |      | Morbillivirus | Narmovirus |
|---------------------------------|------|------|------|------|------|------|------|------|------|------|------|------|-------------|------|---------------|------------|
|                                 |      | MSJ  | BJ   | TJ   | JJ   | MJ   | LJ2  | LJ1  | F    | BL   | K    | B    | G           | HHV  | FMV           | TNV        |
| <b>BtHI-ParaV/<br/>YN2020A</b>  | N    | 65.5 | 49.9 | 50.7 | 48.8 | 45.8 | 51.2 | 43.4 | 42.8 | 55.5 | 55.8 | 56.6 | 49.1        | 44.2 | 46.6          | 41.0       |
|                                 | P    | 63.3 | 55.5 | 56.1 | 53.1 | 55.2 | 53.3 | 58.9 | 57.4 | 53.9 | 52.1 | 56.5 | 52.1        | 26.1 | 48.0          | 45.7       |
|                                 | M    | 77.9 | 62.5 | 63.0 | 62.0 | 61.7 | 64.9 | 65.2 | 68.9 | 66.8 | 68.1 | 71.8 | 69.7        | 48.1 | 46.8          | 46.8       |
|                                 | F    | 54.9 | 50.7 | 51.6 | 50.5 | 51.4 | 50.3 | 50.9 | 50.7 | 50.0 | 51.7 | 52.1 | 53.8        | 39.0 | 38.5          | 39.3       |
|                                 | SH   | 50.1 | 41.5 | 41.8 | 42.1 | 38.4 | –    | –    | –    | –    | –    | –    | –           | –    | –             | –          |
|                                 | TM   | 30.5 | 22.2 | 22.8 | 21.1 | 22.8 | –    | –    | –    | –    | –    | –    | –           | –    | –             | –          |
| <b>BtFi-ParaV/<br/>YN2020K</b>  | G    | 78.5 | 68.2 | 50.5 | 69.9 | 20.4 | 65.5 | 62.5 | 65.3 | 76.8 | 76.4 | 75.7 | 75.0        | 68.6 | 67.2          | 66.3       |
|                                 | L    | 69.6 | 60.2 | 60.4 | 59.0 | 60.6 | 60.7 | 62.7 | 62.4 | 60.3 | 58.2 | 59.3 | 59.9        | 47.2 | 48.7          | 50.1       |
|                                 | N    | 64.8 | 50.1 | 50.4 | 49.1 | 44.4 | 48.5 | 44.4 | 43.1 | 57.4 | 54.5 | 54.7 | 49.6        | 43.7 | 44.7          | 40.9       |
|                                 | P    | 61.0 | 54.4 | 55.4 | 54.5 | 55.5 | 55.4 | 57.4 | 57.3 | 55.5 | 52.5 | 53.4 | 50.4        | 26.5 | 47.9          | 46.6       |
|                                 | M    | 74.7 | 68.9 | 68.6 | 67.6 | 67.8 | 71.3 | 67.8 | 72.9 | 66.8 | 71.0 | 73.1 | 72.1        | 51.1 | 49.5          | 49.2       |
|                                 | F    | 55.4 | 48.8 | 49.0 | 50.2 | 51.2 | 50.5 | 50.3 | 53.0 | 49.7 | 49.5 | 53.3 | 52.6        | 37.1 | 40.2          | 41.3       |
| <b>BtSk-ParaV/<br/>GX2019A</b>  | SH   | 40.1 | 27.6 | 28.1 | 27.0 | 26.5 | –    | –    | –    | –    | –    | –    | –           | –    | –             | –          |
|                                 | TM   | 28.4 | 30.9 | 32.2 | 30.5 | 30.8 | –    | –    | –    | –    | –    | –    | –           | –    | –             | –          |
|                                 | G    | 79.9 | 70.2 | 52.1 | 71.0 | 21.6 | 67.2 | 62.9 | 66.9 | 78.8 | 80.7 | 80.1 | 77.7        | 71.1 | 70.3          | 69.4       |
|                                 | L    | 67.5 | 58.8 | 59.7 | 58.5 | 59.9 | 58.5 | 60.9 | 60.7 | 59.6 | 55.7 | 57.5 | 58.5        | 47.3 | 47.3          | 48.9       |
|                                 | N    | 63.7 | 49.3 | 50.2 | 48.8 | 43.7 | 50.1 | 45.2 | 40.6 | 55.2 | 52.9 | 54.0 | 46.6        | 43.9 | 46.1          | 41.7       |
|                                 | P    | 61.4 | 56.3 | 56.6 | 54.0 | 57.9 | 56.0 | 58.4 | 57.3 | 55.9 | 53.3 | 55.9 | 52.2        | 26.2 | 46.9          | 46.4       |
| <b>BtRs-ParaV/<br/>GD2017E</b>  | M    | 74.5 | 68.1 | 67.3 | 65.7 | 64.1 | 67.0 | 66.2 | 71.3 | 68.9 | 70.5 | 72.1 | 71.0        | 50.3 | 49.2          | 47.3       |
|                                 | F    | 54.5 | 48.8 | 48.6 | 50.5 | 50.5 | 49.3 | 48.4 | 53.3 | 49.3 | 48.3 | 49.7 | 53.5        | 36.7 | 40.4          | 41.8       |
|                                 | SH   | 37.0 | 29.2 | 29.8 | 31.8 | 28.7 | –    | –    | –    | –    | –    | –    | –           | –    | –             | –          |
|                                 | TM   | 29.4 | 30.5 | 31.0 | 29.8 | 30.9 | –    | –    | –    | –    | –    | –    | –           | –    | –             | –          |
|                                 | G    | 78.8 | 69.2 | 51.1 | 70.5 | 21.1 | 66.1 | 62.2 | 66.9 | 77.1 | 79.2 | 78.7 | 77.0        | 70.3 | 69.0          | 68.9       |
|                                 | L    | 67.9 | 59.0 | 59.4 | 58.7 | 59.8 | 59.6 | 61.3 | 61.1 | 58.2 | 55.9 | 57.1 | 57.6        | 48.0 | 47.2          | 48.5       |
| <b>BtRa-ParaV/<br/>YN2020D</b>  | N    | 62.9 | 47.1 | 47.5 | 46.1 | 43.6 | 47.2 | 41.7 | 41.5 | 55.2 | 51.7 | 51.7 | 45.5        | 42.3 | 45.6          | 41.0       |
|                                 | P    | 59.8 | 55.7 | 56.7 | 54.5 | 56.7 | 54.2 | 58.9 | 58.1 | 58.0 | 53.9 | 56.5 | 53.1        | 26.1 | 48.1          | 46.7       |
|                                 | M    | 76.9 | 69.7 | 68.4 | 68.4 | 67.0 | 69.4 | 70.5 | 72.6 | 68.9 | 71.8 | 73.9 | 73.1        | 51.9 | 51.1          | 49.7       |
|                                 | F    | 53.0 | 49.7 | 49.3 | 54.2 | 50.9 | 51.6 | 51.6 | 52.3 | 48.1 | 50.3 | 52.1 | 53.8        | 37.1 | 39.0          | 43.0       |
|                                 | SH   | 38.7 | 31.2 | 31.2 | 31.2 | 28.7 | –    | –    | –    | –    | –    | –    | –           | –    | –             | –          |
|                                 | TM   | 29.9 | 33.8 | 34.0 | 32.3 | 34.1 | –    | –    | –    | –    | –    | –    | –           | –    | –             | –          |
| <b>BtHp-ParaV/<br/>GD2016H</b>  | G    | 79.8 | 69.1 | 50.8 | 70.6 | 20.3 | 66.0 | 62.2 | 66.1 | 77.7 | 78.3 | 77.3 | 76.4        | 70.0 | 69.6          | 68.7       |
|                                 | L    | 66.9 | 59.3 | 60.0 | 58.5 | 60.2 | 60.2 | 63.4 | 61.8 | 60.5 | 55.2 | 57.5 | 59.7        | 46.7 | 47.9          | 48.1       |
|                                 | N    | 64.2 | 46.8 | 47.5 | 47.1 | 42.3 | 47.7 | 43.3 | 43.1 | 56.1 | 52.3 | 51.8 | 47.4        | 43.1 | 46.1          | 41.4       |
|                                 | P    | 60.8 | 57.1 | 57.3 | 56   | 56.2 | 55.4 | 59.2 | 58.6 | 58.0 | 53.6 | 56.1 | 52.2        | 27.1 | 47.5          | 46.4       |
|                                 | M    | 75.8 | 70.2 | 69.1 | 68.4 | 66.0 | 71.0 | 70.2 | 72.6 | 69.9 | 73.1 | 73.4 | 72.6        | 50.0 | 51.6          | 49.7       |
|                                 | F    | 50.3 | 48.8 | 49.0 | 52.1 | 49.7 | 50.9 | 50.5 | 51.2 | 49.7 | 49.8 | 50.7 | 52.3        | 37.4 | 38.6          | 44.2       |
| <b>BtRpu-ParaV/<br/>YN2020H</b> | SH   | 38.4 | 29.0 | 29.2 | 27.9 | 26.5 | –    | –    | –    | –    | –    | –    | –           | –    | –             | –          |
|                                 | TM   | 30.1 | 35.5 | 35.8 | 34.5 | 35.4 | –    | –    | –    | –    | –    | –    | –           | –    | –             | –          |
|                                 | G    | 78.6 | 68.2 | 50.5 | 69.9 | 19.8 | 64.9 | 61.7 | 65.6 | 76.4 | 77.6 | 77.0 | 75.3        | 70.5 | 69.9          | 68.6       |
|                                 | L    | 68.9 | 60.5 | 60.8 | 59.0 | 61.8 | 61.4 | 64.6 | 63.4 | 61.2 | 56.8 | 58.7 | 59.4        | 47.8 | 48.1          | 49.2       |
|                                 | N    | 66.1 | 50.7 | 51.8 | 50.2 | 45.3 | 49.6 | 44.4 | 43.6 | 58.6 | 56.1 | 56.3 | 49.8        | 46.1 | 46.3          | 41.7       |
|                                 | P    | 61.2 | 56.0 | 56.7 | 56.6 | 58.4 | 56.9 | 60.3 | 57.9 | 57.7 | 55.9 | 56.8 | 52.1        | 27.1 | 47.4          | 48.3       |
| <b>BtRpu-ParaV/<br/>YN2020H</b> | M    | 76.1 | 68.9 | 68.6 | 65.4 | 66.0 | 69.7 | 71.3 | 72.3 | 69.9 | 72.1 | 75.0 | 74.2        | 51.3 | 51.3          | 50.5       |
|                                 | F    | 51.2 | 49.3 | 49.1 | 50.0 | 50.9 | 49.8 | 51.0 | 52.8 | 47.4 | 51.0 | 53.3 | 53.7        | 39.3 | 38.1          | 39.2       |
|                                 | SH   | 34.3 | 24.0 | 23.7 | 24.0 | 21.4 | –    | –    | –    | –    | –    | –    | –           | –    | –             | –          |
|                                 | TM   | 32.6 | 32.7 | 33.4 | 31.2 | 32.3 | –    | –    | –    | –    | –    | –    | –           | –    | –             | –          |
|                                 | G    | 80.0 | 69.0 | 51.0 | 70.8 | 20.7 | 66.6 | 62.6 | 65.9 | 78.4 | 78.3 | 78.1 | 76.8        | 70.4 | 69.5          | 68.7       |
|                                 | L    | 68.5 | 60.5 | 61.0 | 59.9 | 61.6 | 61.0 | 63.4 | 62.1 | 61.4 | 57.1 | 59.3 | 59.6        | 47.9 | 47.9          | 49.8       |
| <b>BtRpu-ParaV/<br/>YN2020H</b> | N    | 57.1 | 51.2 | 52.0 | 49.6 | 46.4 | 52.5 | 45.5 | 43.3 | 58.3 | 57.5 | 56.7 | 49.9        | 45.5 | 45.6          | 42.9       |
|                                 | P    | 56.7 | 55.5 | 55.0 | 55.9 | 56.7 | 55.4 | 57.7 | 58.5 | 58.9 | 52.8 | 57.4 | 52.2        | 28.0 | 48.4          | 46.1       |
|                                 | M    | 60.1 | 61.4 | 60.1 | 59.6 | 58.2 | 58.0 | 57.2 | 59.8 | 62.2 | 59.0 | 58.5 | 58.8        | 45.7 | 46.3          | 42.3       |
|                                 | F    | 51.0 | 51.2 | 51.2 | 54.2 | 54.4 | 54.2 | 54.5 | 56.6 | 54.0 | 48.8 | 54.4 | 54.5        | 39.0 | 39.0          | 39.0       |
|                                 | X    | –    | –    | –    | –    | –    | 61.3 | 65.9 | 70.7 | 55.5 | 13.1 | 55.9 | 53.0        | –    | –             | –          |
|                                 | G    | 74.4 | 67.0 | 48.8 | 69.5 | 19.1 | 64.4 | 62.1 | 65.9 | 77.1 | 75.5 | 76.0 | 74.1        | 68.6 | 68.0          | 66.6       |
| L                               | 60.8 | 59.4 | 60.4 | 60.1 | 60.2 | 60.0 | 62.3 | 61.0 | 63.4 | 57.2 | 59.3 | 59.7 | 47.5        | 47.4 | 49.2          |            |

MSJ is *Miniopteran jeilongvirus*, BJ is *Beilong jeilongvirus*, TJ is *Tailam jeilongvirus*, JJ is *Jun jeilongvirus*, MJ is *Myodes jeilongvirus*, LJ2 is *Lophuromys jeilongvirus 2*, LJ1 is *Lophuromys jeilongvirus 1*, F is *Feline paramyxovirus*, BL is *Belerina paramyxovirus*, K is *Kanhgág paramyxovirus*, B is *Boe paramyxovirus*, G is *Guató paramyxovirus*, HHV is *Hendra henipavirus*, FMV is *Feline morbillivirus*, and TNV is *Tupaia narmovirus*.

well as the intracellular and extracellular regions were different. All had one predicted transmembrane helix except for BtRpu-ParaV/YN2020H of L3 which the X encoded a putative protein of 227 amino acids and had no transmembrane region.

3.7. Glycosylation site analysis

The potential N-linked and O-GalNAc glycosylation sites of F and G genes closely related to viral infection were predicted. The amino acid positions of glycosylation sites were listed in [Supplementary Table S5](#). No O-GalNAc glycosylation sites of F genes in BtFi-ParaV/YN2020K, BtSk-ParaV/GX2019A and BtHp-ParaV/GD2016H were found.

4. Discussion

According to the estimate, at least 10,000 virus species can infect humans, but the majority are circulating imperceptibly in wildlife (Carlson et al., 2019; Olival et al., 2017). Some factors include climate changes and increased use of land, which promotes the spillover of zoonotic diseases, resulting in more viral interspecies transmission events from previously geographically located species of wildlife (Carlson et al., 2022; Hoberg and Brooks, 2015; Morales-Castilla et al., 2021). Bats account for most novel viral sharing events and are likely to share viruses that might promote EIDs in humans. Among bat-originated viruses, Hendra virus and Nipah virus under the family *Paramyxoviridae* are

known to infect humans and cause fatal diseases. In 2014, a novel rat henipavirus, Mojiang virus was detected and later confirmed the inability to interact with known paramyxoviral receptors *in vitro* (Rissanen et al., 2017; Wu et al., 2014). Recently, a hypothesized shrew-borne henipavirus named Langya henipavirus associated with a febrile human illness was found in the crowd and animals in contact, further reminds the surveillance of paramyxoviral pathogens need to be characterized (Zhang et al., 2022). To obtain the background information of bat paramyxoviruses in China, bat samples across the mainland were collected and then applied for NGS based virome analysis, a large number of novel paramyxovirus-related sequence reads were found and assigned into the genus *Jeilongvirus*.

Because of limited discoveries, cognized with the genome-constitution of *Jeilongvirus* containing eight ORFs with the order 3'-N-P-M-F-SH-TM-G-L-5', and encoding the TM protein exclusively compared with other genera of *Paramyxoviridae*. However, novel discoveries proposed to this genus in recent years had new hosts including hedgehogs and cats, and some viruses contained only seven major ORFs.

In this study, we discovered 94 paramyxovirus sequences from 22 bat species in China and obtained 17 complete or nearly complete genomes. The results forcefully proposed that the genus *Jeilongvirus* could be divided into four lineages on the basis of phylogenetic analysis of the complete L gene, host range and biochemical criteria, containing new viruses identified in recent studies (de Souza et al., 2021; Sakaguchi et al., 2020; Vanmechelen et al., 2020). The L1 with eight ORFs and L4 with seven ORFs were bat monophyletic; the L2 was co-existed with eight or seven ORFs in rodents and felines; the new L3 with seven ORFs on the trend evolved in bats, hedgehogs and rodents. The *Rhinolophus*, *Scotophilus*, *Miniopterus* and *Myotis* were existed both in L1 and L3, so that the same genus of bats could contain the same virus of different genome structures.

The coding strategy and editing site (TTAAAAAAGGCA) of the *Jeilongvirus* P gene that played an important role in evading the host innate immune system are relatively conserved in the *Henipavirus* and *Morbillivirus*, encoding V or W protein by the addition of one or two single net nontemplated G residues (Jack et al., 2005). The P, V, and W proteins of Nipah virus, a highly lethal pathogen that had been studied well, all block the cellular response to interferon (IFN) by binding to and preventing the tyrosine phosphorylation of signal transducer and activator of transcription 1 (STAT1). The P gene products suppress both the production of and signaling by IFN. Both the V and W proteins block IFN regulatory factor 3-dependent gene expression, V as the major determinant of pathogenesis interacts with the cytoplasmic helicase melanoma differentiation-associated protein 5 (MDA5) and inhibits MDA5-dependent activation of the IFN- $\beta$  promoter, and W modulates the inflammatory host immune response in a manner that determines the disease course (Ciancanelli et al., 2009; Satterfield et al., 2015). However, Cedar virus, which belonged to *Henipavirus* together with Nipah virus and Hendra virus, lacks the pathogenicity. The studies in hamsters, ferrets and guinea pigs confirmed virus replication and production of neutralizing antibodies, but clinical disease was not observed. The reasons that have been verified by experiments of inability to cause disease are receptor specificity to only ephrin B2, cannot suppress the type I IFN response, and the lack of V and W proteins (Marsh et al., 2012; Schountz et al., 2019). The corresponding nucleotide sequence of Cedar virus is 'TAAA-GATCAGGG'. The RNA editing site of L3 and L4 is conserved with L2 of *Jeilongvirus*, but the L1 only found in bats is all replaced by 'TTAAAAAACA', which may indicate that (1) something happens which results in the production of a new coding strategy; (2) the P gene of this bat-related paramyxovirus lacks RNA editing and coding capacity of the V or/and W protein, and influences the pathogenicity just like the Cedar virus. Further experiments are needed to determine the coding strategy, pathogenicity and invasive mechanism of these bat paramyxoviruses.

The infection studies of Beilong virus and J virus of *Jeilongvirus* indicate that they can inhibit STAT1 responses to IFN- $\alpha$ . Both the viruses encode V proteins, but the proteins lack interaction with STAT1/2 and antagonist function toward type I IFN signalling, suggesting that alternative proteins might function as IFN antagonists such as P, C, W, SH and TM (Audsley et al., 2016). Perhaps the functions of P, C and W are similar to the *Henipavirus* and *Morbillivirus* that had not been examined. The SH protein of J virus can inhibit tumor necrosis factor alpha (TNF- $\alpha$ ) production and plays an essential role in blocking apoptosis and virulence. Although there is no sequence homology among SH proteins of mumps virus, respiratory syncytial virus and J virus, their functions are similar (Abraham et al., 2018). The TM protein of J virus is a type II integral membrane protein and required with F and G for efficient cell-to-cell fusion, but does not affect replication in tissue culture cells (Li et al., 2015). All SH, TM and X proteins of *Jeilongvirus* have one predicted transmembrane helix except for BtRpu-ParaV/YN2020H of L3 that has no transmembrane region indicated functional difference between X and TM. More attention should be focused on these novel paramyxoviruses with significant changes.

The host and region switches were tentatively established and the Bayesian factors were calculated based on available data. Combining the information of hosts and regions, the approximately evolutionary trend was revealed. The genus *Jeilongvirus* may have originated from *Mus* in Australia, then transmitted to bats and rodents in Africa, Asia and Europe, and finally to bats and rodents in America. Felines and hedgehogs were most likely the intermediate hosts from *Scotophilus* of bats rather than rodents. The bat colony was partial to interior, and rodent colony was exported based on this trend. However, it is important to note that: (1) new studies focused on *Jeilongvirus* genus were insufficient in host range and territorial scope; (2) most samples were tested by the consensus degenerate primers to obtain partial L sequences instead of complete genomes; (3) sampling imbalance in different hosts from the same region or different regions from the same host influenced the transmitting trend; (4) the accurate origin and transmission time were not pointed out, and many important switch-intermediate-nodes were not found. Due to the limitations of current data, more extensive survey of animal paramyxoviruses in under sampling hosts and regions are needed to further investigate the accurate origin and evolutionary route.

## 5. Conclusions

In this study, we conducted systematic survey of bat paramyxoviruses in China. A total of 94 paramyxovirus sequences were identified from 22 bat species, and 17 complete or nearly complete genomes were obtained among them. The genus *Jeilongvirus* could be divided into four lineages with the evolution or predicted trend from *Mus* in Australia, to bats and rodents in Africa, Asia and Europe, and finally to bats and rodents in America. Although there is no evidence that bat jeilongvirus poses a threat to human health at present, the finding in this study is still helpful for us to understand the relationships between distribution and cross-species transmission of paramyxoviruses and the migration and co-roosting of their broad distributed host. Further experiments are needed to determine the pathogenicity and invasive mechanism of these jeilongviruses to bats or other related animal hosts.

## Data availability

Datasets generated and analyzed during the current study are available in this published article (and its supplementary information files).

## Ethics statement

Animals were treated according to the guidelines of the Regulations for the Administration of Laboratory Animals (Decree No. 2 of the State



Science and Technology Commission of the People's Republic of China, 1988). Sampling procedures were approved by the Ethics Committee of the Institute of Pathogen Biology, Chinese Academy of Medical Sciences & Peking Union Medical College (Approval number: IPB EC20100415).

### Author contributions

Haoxiang Su: conceptualization, data curation, formal analysis, investigation, validation, visualization, writing - original draft. Yuyang Wang: data curation, formal analysis, software, visualization. Yelin Han: data curation, validation, visualization. Qi Jin: conceptualization, resources, supervision, writing - review & editing. Fan Yang: conceptualization, supervision, writing - review & editing. Zhiqiang Wu: conceptualization, funding acquisition, resources, supervision, writing - review & editing.

### Conflict of interest

The authors declare that they have no competing interests.

### Acknowledgments

This work was supported by Beijing Natural Science Foundation (Grant No. M21002), the National Key R&D Program of China (Grant No. 2021YFC2300902 and 2022YFE0210300), the CAMS Innovation Fund for Medical Sciences (Grant No. 2021-I2M-1-038 and 2022-I2M-CoV19-002), Science & Technology Fundamental Resources Investigation Program (Grant No. 2022FY100901), the Non-profit Central Research Institute Fund of Chinese Academy of Medical Sciences (2019PT310029), and the Fundamental Research Funds for the Central Universities (Grant No. 3332021092).

### Appendix A. Supplementary data

Supplementary data to this article can be found online at <https://doi.org/10.1016/j.virs.2023.01.002>.

### References

- Abraham, M., Arroyo-Diaz, N.M., Li, Z., Zengel, J., Sakamoto, K., He, B., 2018. Role of small Hydrophobic protein of J paramyxovirus in Virulence. *J. Virol.* 92, e00653-18.
- Albarino, C.G., Foltzer, M., Towner, J.S., Rowe, L.A., Campbell, S., Jaramillo, C.M., Bird, B.H., Reeder, D.M., Vodzak, M.E., Rota, P., Metcalfe, M.G., Spiropoulou, C.F., Knust, B., Vincent, J.P., Ftrace, M.A., Nichol, S.T., Rollin, P.E., Stroher, U., 2014. Novel paramyxovirus associated with severe acute febrile disease, South Sudan and Uganda, 2012. *Emerg. Infect. Dis.* 20, 211–216.
- Alkhovsky, S., Butenko, A., Eremyan, A., Shchetinin, A., 2018. Genetic characterization of bank vole virus (BaVV), a new paramyxovirus isolated from kidneys of bank voles in Russia. *Arch. Virol.* 163, 755–759.
- Audsley, M.D., Marsh, G.A., Lieu, K.G., Tachedjian, M., Joubert, D.A., Wang, L.F., Jans, D.A., Moseley, G.W., 2016. The immune evasion function of J and Beilong virus V proteins is distinct from that of other paramyxoviruses, consistent with their inclusion in the proposed genus Jeilongvirus. *J. Gen. Virol.* 97, 581–592.
- Baele, G., Lemey, P., Bedford, T., Rambaut, A., Suchard, M.A., Alekseyenko, A.V., 2012. Improving the accuracy of Demographic and molecular clock model Comparison while Accommodating phylogenetic Uncertainty. *Mol. Biol. Evol.* 29, 2157–2167.
- Baele, G., Li, W.L., Drummond, A.J., Suchard, M.A., Lemey, P., 2013. Accurate model selection of relaxed molecular clocks in Bayesian phylogenetics. *Mol. Biol. Evol.* 30, 239–243.
- Baker, K.S., Tachedjian, M., Barr, J., Marsh, G.A., Todd, S., Cramer, G., Cramer, S., Smith, I., Holmes, C.E.G., Suu-Ire, R., Fernandez-Loras, A., Cunningham, A.A., Wood, J.L.N., Wang, L.F., 2020. Achimota Pararubulavirus 3: a new bat-Derived paramyxovirus of the genus Pararubulavirus. *Viruses* 12, 1236.
- Bielejec, F., Baele, G., Vrancken, B., Suchard, M.A., Rambaut, A., Lemey, P., 2016. Spread3: Interactive Visualization of Spatiotemporal history and trait evolutionary Processes. *Mol. Biol. Evol.* 33, 2167–2169.
- Bowden, T.R., Bingham, J., Harper, J.A., Boyle, D.B., 2012. Menangle virus, a pteropid bat paramyxovirus infectious for pigs and humans, exhibits tropism for secondary lymphoid organs and intestinal epithelium in weaned pigs. *J. Gen. Virol.* 93, 1007–1016.
- Branche, A.R., Falsely, A.R., 2016. Parainfluenza virus infection. *Semin. Respir. Crit. Care Med.* 37, 538–554.
- Brooks, F., Wood, A.R., Thomson, J., Deane, D., Everest, D.J., McInnes, C.J., 2014. Preliminary characterisation of Pentlands paramyxovirus-1,-2 and-3, three new paramyxoviruses of rodents. *Vet. Microbiol.* 170, 391–397.
- Burroughs, A.L., Tachedjian, M., Cramer, G., Durr, P.A., Marsh, G.A., Wang, L.F., 2015. Complete genome sequence of teviot paramyxovirus, a novel rubulavirus isolated from fruit bats in Australia. *Genome Announc.* 3, e00177-15.
- Calisher, C.H., Childs, J.E., Field, H.E., Holmes, K. v, Schountz, T., 2006. Bats: important reservoir hosts of emerging viruses. *Clin. Microbiol. Rev.* 19, 531–545.
- Carlson, C.J., Alberty, G.F., Merow, C., Trisos, C.H., Zipfel, C.M., Eskew, E.A., Olival, K.J., Ross, N., Bansal, S., 2022. Climate change increases cross-species viral transmission risk. *Nature* 607, 555–562.
- Carlson, C.J., Zipfel, C.M., Garnier, R., Bansal, S., 2019. Global estimates of mammalian viral diversity accounting for host sharing. *Nat Ecol Evol* 3, 1070–1075.
- Chen, C., Chen, H., Zhang, Y., Thomas, H.R., Frank, M.H., He, Y., Xia, R., 2020. TBtools: an Integrative Toolkit Developed for interactive analyses of Big Biological data. *Mol. Plant* 13, 1194–1202.
- Chen, L.H., Liu, B., Wu, Z.Q., Jin, Q., Yang, J., 2017. DRodVir: a resource for exploring the virome diversity in rodents. *J. Genet. Genomics* 44, 259–264.
- Chen, L.H., Liu, B., Yang, J., Jin, Q., 2014. DBatVir: the database of bat-associated viruses. *Database-the Journal of Biological Databases and Curation* 2014, bau021.
- Choi, E.J., Ortega, V., Aguilar, H.C., 2020. Feline morbillivirus, a new paramyxovirus possibly associated with feline kidney disease. *Viruses* 12, 501.
- Ciancanelli, M.J., Volchkova, V.A., Shaw, M.L., Volchkov, V.E., Basler, C.F., 2009. Nipah virus sequesters inactive STAT1 in the nucleus via a P gene-encoded mechanism. *J. Virol.* 83, 7828–7841.
- de Souza, W.M., Fumagalli, M.J., Carrera, J.P., de Araujo, J., Cardoso, J.F., de Carvalho, C., Durigon, E.L., Queiroz, L.H., Faria, N.R., Murcia, P.R., Figueiredo, L.T.M., 2021. Paramyxoviruses from neotropical bats suggest a novel genus and nephrotropism. *Infect. Genet. Evol.* 95, 105041.
- Drexler, J.F., Corman, V.M., Muller, M.A., Maganga, G.D., Vallo, P., Binger, T., Gloza-Rausch, F., Cottontail, V.M., Rasche, A., Yordanov, S., Seebens, A., Knornschild, M., Oppong, S., Adu Sarkodie, Y., Pongombo, C., Lukashev, A.N., Schmidt-Chanasit, J., Stocker, A., Carneiro, A.J., Erbar, S., Maisner, A., Fronhoffs, F., Buettner, R., Kalko, E.K., Kruppa, T., Franke, C.R., Kallies, R., Yandoko, E.R., Herrler, G., Reusken, C., Hassanin, A., Kruger, D.H., Matthee, S., Ulrich, R.G., Leroy, E.M., Drosten, C., 2012. Bats host major mammalian paramyxoviruses. *Nat. Commun.* 3, 796.
- Forth, L.F., Konrath, A., Klose, K., Schlottau, K., Hoffmann, K., Ulrich, R.G., Hoper, D., Pohlmann, A., Beer, M., 2018. A novel squirrel Respirivirus with putative zoonotic potential. *Viruses* 10, 373.
- Halpin, K., Hyatt, A.D., Fogarty, R., Middleton, D., Bingham, J., Epstein, J.H., Rahman, S.A., Hughes, T., Smith, C., Field, H.E., Daszak, P., Grp, H.E.R., 2011. Pteropid bats are confirmed as the reservoir hosts of henipaviruses: a comprehensive experimental study of virus transmission. *Am. J. Trop. Med. Hyg.* 85, 946–951.
- Henrickson, K.J., 2003. Parainfluenza viruses. *Clin. Microbiol. Rev.* 16, 242–264.
- Hoang, D.T., Chernomor, O., von Haeseler, A., Minh, B.Q., Vinh, L.S., 2018. UFBoot2: Improving the Ultrafast Bootstrap approximation. *Mol. Biol. Evol.* 35, 518–522.
- Hoberg, E.P., Brooks, D.R., 2015. Evolution in action: climate change, biodiversity dynamics and emerging infectious disease. *Philos. Trans. R. Soc. Lond. B Biol. Sci.* 370, 20130553.
- Hviid, A., Rubin, S., Muhlemann, K., 2008. Mumps. *Lancet* 371, 932–944.
- Hyndman, T.H., Marschang, R.E., Wellehan, J.F.X., Nicholls, P.K., 2012. Isolation and molecular identification of Sunshine virus, a novel paramyxovirus found in Australian snakes. *Infect. Genet. Evol.* 12, 1436–1446.
- Jack, P.J., Boyle, D.B., Eaton, B.T., Wang, L.F., 2005. The complete genome sequence of J virus reveals a unique genome structure in the family Paramyxoviridae. *J. Virol.* 79, 10690–10700.
- Johnson, R.I., Tachedjian, M., Rowe, B., Clayton, B.A., Layton, R., Bergfeld, J., Wang, L.F., Marsh, G.A., 2018. Alston virus, a novel paramyxovirus isolated from bats causes Upper respiratory Tract infection in experimentally Challenged ferrets. *Viruses* 10, 675.
- Kalyaanamoorthy, S., Minh, B.Q., Wong, T.K.F., von Haeseler, A., Jermini, L.S., 2017. ModelFinder: fast model selection for accurate phylogenetic estimates. *Nat. Methods* 14, 587–589.
- Katoh, K., Standley, D.M., 2013. MAFFT multiple sequence alignment software version 7: improvements in performance and usability. *Mol. Biol. Evol.* 30, 772–780.
- Lambeth, L.S., Yu, M., Anderson, D.E., Cramer, G., Eaton, B.T., Wang, L.F., 2009. Complete genome sequence of Nariva virus, a rodent paramyxovirus. *Arch. Virol.* 154, 199–207.
- Larsen, B.B., Gryseels, S., Otto, H.W., Worobey, M., 2021. Evolution and diversity of bat and rodent Paramyxoviruses from North America. *J. Virol.* 96, e0109821.
- Lau, S.K., Woo, P.C., Li, K.S., Huang, Y., Tsoi, H.W., Wong, B.H., Wong, S.S., Leung, S.Y., Chan, K.H., Yuen, K.Y., 2005. Severe acute respiratory syndrome coronavirus-like virus in Chinese horseshoe bats. *Proc. Natl. Acad. Sci. U. S. A.* 102, 14040–14045.
- Lau, S.K., Woo, P.C., Wong, B.H., Wong, A.Y., Tsoi, H.W., Wang, M., Lee, P., Xu, H., Poon, R.W., Guo, R., Li, K.S., Chan, K.H., Zheng, B.J., Yuen, K.Y., 2010. Identification and complete genome analysis of three novel paramyxoviruses, Tuhoko virus 1, 2 and 3, in fruit bats from China. *Virology* 404, 106–116.
- Lau, S.K.P., Woo, P.C.Y., Wu, Y., Wong, A.Y.P., Wong, B.H.L., Lau, C.C.Y., Fan, R.Y.Y., Cai, J.P., Tsoi, H.W., Chan, K.H., Yuen, K.Y., 2013. Identification and characterization of a novel paramyxovirus, porcine parainfluenza virus 1, from deceased pigs. *J. Gen. Virol.* 94, 2184–2190.
- Leal, E., Liu, C., Zhao, Z., Deng, Y., Villanova, F., Liang, L., Li, J., Cui, S., 2019. Isolation of a Divergent strain of Bovine parainfluenza virus type 3 (BPiV3) infecting cattle in China. *Viruses* 11, 489.

- Lee, S.H., No, J.S., Kim, K., Budhathoki, S., Park, K., Lee, G.Y., Cho, S., Kim, B.H., Cho, S., Kim, J., Lee, J., Cho, S.H., Kim, H.C., Klein, T.A., Uhm, C.S., Kim, W.K., Song, J.W., 2021. Novel Paju Apodemus paramyxovirus 1 and 2, harbored by Apodemus agrarius in the Republic of Korea. *Virology* 562, 40–49.
- Lemey, P., Rambaut, A., Drummond, A.J., Suchard, M.A., 2009. Bayesian phylogeography finds its roots. *PLoS Comput. Biol.* 5, e1000520.
- Leroy, E.M., Kumulungui, B., Pourrut, X., Rouquet, P., Hassanin, A., Yaba, P., Delicat, A., Paweska, J.T., Gonzalez, J.P., Swanepoel, R., 2005. Fruit bats as reservoirs of Ebola virus. *Nature* 438, 575–576.
- Letko, M., Seifert, S.N., Olival, K.J., Plowright, R.K., Munster, V.J., 2020. Bat-borne virus diversity, spillover and emergence. *Nat. Rev. Microbiol.* 18, 461–471.
- Li, W., Mao, L., Cheng, S., Wang, Q., Huang, J., Deng, J., Wang, Z., Zhang, W., Yang, L., Hao, F., Ding, Y., Sun, Y., Wei, J., Jiang, P., Jiang, J., 2014. A novel parainfluenza virus type 3 (PIV3) identified from goat herds with respiratory diseases in eastern China. *Vet. Microbiol.* 174, 100–106.
- Li, Z., Hung, C., Paterson, R.G., Michel, F., Fuentes, S., Place, R., Lin, Y., Hogan, R.J., Lamb, R.A., He, B., 2015. Type II integral membrane protein, TM of J paramyxovirus promotes cell-to-cell fusion. *Proc. Natl. Acad. Sci. U. S. A.* 112, 12504–12509.
- Marsh, G.A., de Jong, C., Barr, J.A., Tachedjian, M., Smith, C., Middleton, D., Yu, M., Todd, S., Foord, A.J., Haring, V., Payne, J., Robinson, R., Broz, L., Cramer, G., Field, H.E., Wang, L.F., 2012. Cedar virus: a novel Henipavirus isolated from Australian bats. *PLoS Pathog.* 8, e1002836.
- Marsh, G.A., Wang, L.F., 2012. Hendra and Nipah viruses: why are they so deadly? *Curr Opin Virol* 2, 242–247.
- Memish, Z.A., Mishra, N., Olival, K.J., Fagbo, S.F., Kapoor, V., Epstein, J.H., Alhakeem, R., Durosinloun, A., al Asmari, M., Islam, A., Kapoor, A., Briese, T., Daszak, P., al Rabeeah, A.A., Lipkin, W.I., 2013. Middle East respiratory syndrome coronavirus in bats, Saudi Arabia. *Emerg. Infect. Dis.* 19, 1819–1823.
- Middleton, D., 2014. Hendra virus. *Vet Clin North Am Equine Pract* 30, 579–589.
- Miller, P.J., Boyle, D.B., Eaton, B.T., Wang, L.F., 2003. Full-length genome sequence of Mossman virus, a novel paramyxovirus isolated from rodents in Australia. *Virology* 317, 330–344.
- Morales-Castilla, I., Pappalardo, P., Farrell, M.J., Aguirre, A.A., Huang, S., Gehman, A.M., Dallas, T., Gravel, D., Davies, T.J., 2021. Forecasting parasite sharing under climate change. *Philos. Trans. R. Soc. Lond. B Biol. Sci.* 376, 20200360.
- Moss, W.J., 2017. Measles. *Lancet* 390, 2490–2502.
- Nguyen, L.T., Schmidt, H.A., von Haeseler, A., Minh, B.Q., 2015. IQ-TREE: a fast and effective stochastic algorithm for estimating maximum-likelihood phylogenies. *Mol. Biol. Evol.* 32, 268–274.
- Noh, J.Y., Jeong, D.G., Yoon, S.W., Kim, J.H., Choi, Y.G., Kang, S.Y., Kim, H.K., 2018. Isolation and characterization of novel bat paramyxovirus B16-40 potentially belonging to the proposed genus Shaanvirus. *Sci. Rep.* 8, 12533.
- Olival, K.J., Hosseini, P.R., Zambrana-Torrel, C., Ross, N., Bogich, T.L., Daszak, P., 2017. Host and viral traits predict zoonotic spillover from mammals. *Nature* 546, 646–650.
- Rambaut, A., Drummond, A.J., Xie, D., Baele, G., Suchard, M.A., 2018. Posterior Summarization in Bayesian phylogenetics using Tracer 1.7. *Syst. Biol.* 67, 901–904.
- Rambaut, A., Lam, T.T., Carvalho, L.M., Pybus, O.G., 2016. Exploring the temporal structure of heterochronous sequences using TempEst (formerly Path-O-Gen). *Virus Evol* 2, vew007.
- Rima, B., Balkema-Buschmann, A., Dundon, W.G., Duprex, P., Easton, A., Fouchier, R., Kurath, G., Lamb, R., Lee, B., Rota, P., Wang Ictv Report Consortium, L., 2019. ICTV virus Taxonomy profile: Paramyxoviridae. *J. Gen. Virol.* 100, 1593–1594.
- Rissanen, I., Ahmed, A.A., Azarm, K., Beaty, S., Hong, P., Nambulli, S., Duprex, W.P., Lee, B., Bowden, T.A., 2017. Idiosyncratic Mojiang virus attachment glycoprotein directs a host-cell entry pathway distinct from genetically related henipaviruses. *Nat. Commun.* 8, 16060.
- Sakaguchi, S., Nakagawa, S., Mitsuhashi, S., Ogawa, M., Sugiyama, K., Tamukai, K., Koide, R., Katayama, Y., Nakano, T., Makino, S., Imanishi, T., Miyazawa, T., Mizutani, T., 2020. Molecular characterization of feline paramyxovirus in Japanese cat populations. *Arch. Virol.* 165, 413–418.
- Satterfield, B.A., Cross, R.W., Fenton, K.A., Agans, K.N., Basler, C.F., Geisbert, T.W., Mire, C.E., 2015. The immunomodulating V and W proteins of Nipah virus determine disease course. *Nat. Commun.* 6, 7483.
- Schountz, T., Campbell, C., Wagner, K., Rovnak, J., Martellaro, C., DeBuysscher, B.L., Feldmann, H., Prescott, J., 2019. Differential innate immune responses Elicited by Nipah virus and Cedar virus Correlate with Disparate in Vivo pathogenesis in hamsters. *Viruses* 11, 291.
- Sieg, M., Heenemann, K., Ruckner, A., Burgener, I., Oechtering, G., Vahlenkamp, T.W., 2015. Discovery of new feline paramyxoviruses in domestic cats with chronic kidney disease. *Virus Gene.* 51, 294–297.
- Smith, I., Wang, L.F., 2013. Bats and their virome: an important source of emerging viruses capable of infecting humans. *Curr Opin Virol* 3, 84–91.
- Suchard, M.A., Lemey, P., Baele, G., Ayres, D.L., Drummond, A.J., Rambaut, A., 2018. Bayesian phylogenetic and phylodynamic data integration using BEAST 1.10. *Virus Evol* 4, vey016.
- Swanepoel, R., Smit, S.B., Rollin, P.E., Formenty, P., Leman, P.A., Kemp, A., Burt, F.J., Grobelaar, A.A., Croft, J., Bausch, D.G., Zeller, H., Leirs, H., Braack, L.E., Libande, M.L., Zaki, S., Nichol, S.T., Ksiazek, T.G., Paweska, J.T., International, S., 2007. Technical Committee for Marburg Hemorrhagic Fever Control in the Democratic Republic of, C., Studies of reservoir hosts for Marburg virus. *Emerg. Infect. Dis.* 13, 1847–1851.
- Tong, S., Chern, S.W., Li, Y., Pallansch, M.A., Anderson, L.J., 2008. Sensitive and broadly reactive reverse transcription-PCR assays to detect novel paramyxoviruses. *J. Clin. Microbiol.* 46, 2652–2658.
- Vanmechelen, B., Bletsa, M., Laenen, L., Lopes, A.R., Vergote, V., Beller, L., Deboutte, W., Korva, M., Avsic Zupanc, T., Gouy de Bellocq, J., Gryseels, S., Leirs, H., Lemey, P., Vrancken, B., Maes, P., 2018. Discovery and genome characterization of three new Jeilongviruses, a lineage of paramyxoviruses characterized by their unique membrane proteins. *BMC Genom.* 19, 617.
- Vanmechelen, B., Meurs, S., Zisi, Z., Gouy de Bellocq, J., Bletsa, M., Lemey, P., Maes, P., 2021. Genome sequence of Ruloma virus, a novel paramyxovirus clustering Basally to members of the genus jeilongvirus. *Microbiol. Resour. Announc.* 10, e00325-21.
- Vanmechelen, B., Vergote, V., Merino, M., Verbeken, E., Maes, P., 2020. Common occurrence of Belerina virus, a novel paramyxovirus found in Belgian hedgehogs. *Sci. Rep.* 10, 19341.
- Wang, L.F., Shi, Z., Zhang, S., Field, H., Daszak, P., Eaton, B.T., 2006. Review of bats and SARS. *Emerg. Infect. Dis.* 12, 1834–1840.
- Woo, P.C., Lau, S.K., Wong, B.H., Wong, A.Y., Poon, R.W., Yuen, K.Y., 2011. Complete genome sequence of a novel paramyxovirus, Tailam virus, discovered in Sikkim rats. *J. Virol.* 85, 13473–13474.
- Wu, Z., Han, Y., Wang, Y., Liu, B., Zhao, L., Zhang, J., Su, H., Zhao, W., Liu, L., Bai, S., Dong, J., Sun, L., Zhu, Y., Zhou, S., Song, Y., Sui, H., Yang, J., Wang, J., Zhang, S., Qian, Z., Jin, Q., 2022. A comprehensive survey of bat sarbecoviruses across China in relation to the origins of SARS-CoV and SARS-CoV-2. *Nat. Sci. Rev. https://doi.org/10.1093/nsr/nwac213 nwac213*.
- Wu, Z., Ren, X., Yang, L., Hu, Y., Yang, J., He, G., Zhang, J., Dong, J., Sun, L., Du, J., Liu, L., Xue, Y., Wang, J., Yang, F., Zhang, S., Jin, Q., 2012. Virome analysis for identification of novel mammalian viruses in bat species from Chinese provinces. *J. Virol.* 86, 10999–11012.
- Wu, Z., Yang, L., Ren, X., He, G., Zhang, J., Yang, J., Qian, Z., Dong, J., Sun, L., Zhu, Y., Du, J., Yang, F., Zhang, S., Jin, Q., 2016. Deciphering the bat virome catalog to better understand the ecological diversity of bat viruses and the bat origin of emerging infectious diseases. *ISME J.* 10, 609–620.
- Wu, Z., Yang, L., Yang, F., Ren, X., Jiang, J., Dong, J., Sun, L., Zhu, Y., Zhou, H., Jin, Q., 2014. Novel Henipa-like virus, Mojiang paramyxovirus, in rats, China, 2012. *Emerg. Infect. Dis.* 20, 1064–1066.
- Wu, Z.Q., Han, Y.L., Liu, B., Li, H.Y., Zhu, G.J., Latinne, A., Dong, J., Sun, L.L., Su, H.X., Liu, L.G., Du, J., Zhou, S.Y., Chen, M.X., Kritiyakan, A., Jittapalpong, S., Chaisiri, K., Buchy, P., Duong, V., Yang, J.A., Jiang, J.Y., Xu, X., Zhou, H.N., Yang, F., Irwin, D.M., Morand, S., Daszak, P., Wang, J.W., Jin, Q., 2021. Decoding the RNA viromes in rodent lungs provides new insight into the origin and evolutionary patterns of rodent-borne pathogens in Mainland Southeast Asia. *Microbiome* 9, 18.
- Wu, Z., Lu, L., Du, J., Yang, L., Ren, X.W., Liu, B., Jiang, J.Y., Yang, J., Dong, J., Sun, L.L., Zhu, Y.F., Li, Y.H., Zheng, D.D., Zhang, C., Su, H.X., Zheng, Y.T., Zhou, H.N., Zhu, G.J., Li, H.Y., Chmura, A., Yang, F., Daszak, P., Wang, J.W., Liu, Q.Y., Jin, Q., 2018. Comparative analysis of rodent and small mammal viromes to better understand the wildlife origin of emerging infectious diseases. *Microbiome* 6, 178.
- Yang, J., Yang, F., Ren, L.L., Xiong, Z.H., Wu, Z.Q., Dong, J., Sun, L.L., Zhang, T., Hu, Y.F., Du, J., Wang, J.W., Jin, Q., 2011. Unbiased Parallel detection of viral pathogens in clinical samples by Use of a Metagenomic Approach. *J. Clin. Microbiol.* 49, 3463–3469.
- Zhang, X.A., Li, H., Jiang, F.C., Zhu, F., Zhang, Y.F., Chen, J.J., Tan, C.W., Anderson, D.E., Fan, H., Dong, L.Y., Li, C., Zhang, P.H., Li, Y., Ding, H., Fang, L.Q., Wang, L.F., Liu, W., 2022. A zoonotic henipavirus in febrile Patients in China. *N. Engl. J. Med.* 387, 470–472.